

# Accelerating Universe in Hybrid and Logarithmic Teleparallel Gravity

Sanjay Mandal<sup>1</sup>, Snehasish Bhattacharjee<sup>2</sup>, S. K. J. Pacif<sup>3</sup>, P.K. Sahoo<sup>1</sup>

<sup>1</sup> Department of Mathematics, Birla Institute of Technology and Science-Pilani, Hyderabad Campus, Hyderabad-500078, India

<sup>2</sup> Department of Astronomy, Osmania University, Hyderabad-500007, India and

<sup>3</sup> Department of Mathematics, School of Advanced Sciences,  
Vellore Institute of Technology, Vellore 632014, Tamil Nadu, India.

Teleparallel gravity is a modified theory of gravity for which the Ricci scalar  $R$  of the underlying geometry in the action is replaced by an arbitrary functional form of torsion scalar  $T$ . In doing so, cosmology in  $f(T)$  gravity becomes greatly simplified owing to the fact that  $T$  contains only the first derivatives of the vierbeins. The article exploits this appealing nature of  $f(T)$  gravity and present cosmological scenarios from hybrid and logarithmic teleparallel gravity models of the form  $f = e^{mT} T^n$  and  $f = D \log(bT)$  respectively, where  $m$ ,  $n$ ,  $D$  and  $b$  are free parameters constrained to suffice the late time acceleration. We employ a well motivated parametrization of the deceleration parameter having just one degree of freedom constrained with a  $\chi^2$  test from 57 data points of Hubble data set in the redshift range  $0.07 < z < 2.36$ , to obtain the expressions of pressure, density and EoS parameter for both the teleparallel gravity models and study their temporal evolution. We find the deceleration parameter to experience a signature flipping for the  $\chi^2$  value of the free parameter at  $z_{tr} \simeq 0.6$  which is consistent with latest Planck measurements. Next, we present few geometric diagnostics of this parametrization to understand the nature of dark energy and its deviation from the  $\Lambda$ CDM cosmology. Finally, we study the energy conditions to check the consistency of the parameter spaces for both the teleparallel gravity models. We find the SEC to violate for both the models which is an essential recipe to obtain an accelerating universe.

PACS numbers: 04.50.Kd

## I. INTRODUCTION

Several Observations reveal that the universe is accelerating for the very second time in its 13.7 billion year long lifetime [1]. It has now been agreed that a cosmological entity with almost three-quarters of the energy budget of the universe coupled with a EoS parameter  $\omega \simeq -1$  is required to suffice the observations. In this spirit, several interesting proposals have been reported to expound this conundrum [2].

One of the most interesting proposal refuting the existence of dark energy are the ‘modified theories of gravity’. In modified gravity theories, dark energy is purely geometric in nature and is connected to novel dynamical terms following modification of the Einstein-Hilbert action [3]. Many such theories such as  $f(R)$  gravity,  $f(G)$  gravity,  $f(R, T)$  gravity, etc have widespread use in modern cosmology (For a recent review on modified gravity see [4]. Also see [5] for some interesting cosmological applications of modified gravity).

Teleparallel gravity is a well established and well motivated modified theory of gravity inspired from  $f(R)$  gravity [6] (See [7] for a review on teleparallel gravity). In teleparallel gravity, the Ricci scalar  $R$  of the underlying geometry in the action is replaced by an arbitrary functional form of torsion scalar  $T$ . Thus, in teleparallel gravity, instead of using the torsionless Levi-Civita connection (which is usually assumed in GR), the curvatureless Weitzenböck connection is employed in which the corresponding dynamical fields are the four linearly independent verbeins, and  $T$  is related to the antisymmetric connection following from the non-holonomic basis [3, 8].

Linear  $f(T)$  gravity models are the teleparallel equivalent of GR (TEGR) [9]. Nonetheless,  $f(T)$  gravity differ significantly from  $f(R)$  gravity in the fact that the field equations in  $f(T)$  gravity are always at second-order compared to the usual fourth-order in  $f(R)$  gravity. This owes to the fact that the torsion scalar contains only the first derivatives of the vierbeins and thus makes cosmology in  $f(T)$  gravity much simpler. However, Despite being a second-order theory, very few exact solutions of the field equations have been reported in literature. Power law solutions in FLRW spacetime have been reported in [12], while for anisotropic spacetimes in [10]. Solutions for Bianchi I spacetime and static spherically spacetimes can be found in [3] and [11] respectively.

Since cosmology in  $f(T)$  gravity is much simpler compared to other modified gravity theories, it has been employed to model inflation [13], late time acceleration [14] and big bounce [15]. The instability epochs of self-gravitating objects coupled with anisotropic radiative matter content and the instability of cylindrical compact object in  $f(T)$  gravity have been discussed in Ref. [16, 17].

The manuscript is organized as follows: In Section II we present an overview of  $f(T)$  gravity. In Section III we describe the kinematic variables obtained from a parametrization of deceleration parameter used to obtain the exact solutions of the field equations. In Section IV we present the hybrid and logarithmic teleparallel gravity models and obtain the expressions of pressure, density and EoS parameter. In Section V we present some geometric diagnostics of the parametrization of deceleration parameter. In Section VI we study the energy conditions for both the teleparallel gravity models. In Section VII we obtain some observational bounds on the free parameters of the parametrization by performing a chi-square test using Hubble datasets with 57 datapoints, Supernovae datasets consisting of 580 data points from Union2.1 compilation datasets and Baryonic Acoustic Oscillation (BAO) datasets. Finally, in Section

VIII we present our results and conclusions.

## II. OVERVIEW OF $f(T)$ GRAVITY

The action in teleparallel gravity is represented as

$$S = \frac{1}{16\pi G} \int [T + f(T)] e d^4 x, \quad (1)$$

where  $e = \det(e_\mu^i) = \sqrt{-g}$  and  $G$  is Newtonian gravitational constant. The gravitational field in this framework arises due to torsion defined as

$$T_{\mu\nu}^\gamma \equiv e_i^\gamma (\partial_\mu e_\nu^i - \partial_\nu e_\mu^i). \quad (2)$$

The contracted form of torsion tensor reads

$$T \equiv \frac{1}{4} T^{\gamma\mu\nu} T_{\gamma\mu\nu} + \frac{1}{2} T^{\gamma\mu\nu} T_{\nu\mu\gamma} - T_{\gamma\mu}^\gamma T_\nu^{\nu\mu}. \quad (3)$$

varying the action  $S + L_m$ , where  $L_m$  represent the matter Lagrangian yields the field equations as

$$e^{-1} \partial_\mu (e e_i^\gamma S_\gamma^{\mu\nu}) (1 + f_T) - (1 + f_T) e_i^\lambda T_{\mu\lambda}^\gamma S_\gamma^{\nu\mu} + e_i^\gamma S_\gamma^{\mu\nu} \partial_\mu (T) f_{TT} + \frac{1}{4} e_i^\nu [T + f(T)] = \frac{k^2}{2} e_i^\gamma T_\gamma^{(M)\nu}, \quad (4)$$

where  $f_T = df(T)/dT$ ,  $f_{TT} = d^2f(T)/dT^2$ , the ‘‘superpotential’’ tensor  $S_\gamma^{\mu\nu}$  written in terms of cotorsion  $K_\gamma^{\mu\nu} = -\frac{1}{2}(T_\gamma^{\mu\nu} - T_\alpha^{\nu\mu} - T_\alpha^{\mu\nu})$  as  $S_\gamma^{\mu\nu} = \frac{1}{2}(K_\gamma^{\mu\nu} + \delta_\gamma^\mu T_\alpha^{\alpha\nu} - \delta_\gamma^\nu T_\alpha^{\alpha\mu})$  and  $T_\gamma^{(M)\nu}$  represents the energy-momentum tensor to the matter Lagrangian  $L_m$ . For a flat FLRW universe with the metric denoted as

$$ds^2 = dt^2 - a^2(t) dx^\mu dx^\nu, \quad (5)$$

where  $a(t)$  the scale factor, gives

$$e_\mu^i = \text{diag}(1, a, a, a). \quad (6)$$

Employing (5) into the field equation (4), the modified Friedman equations reads

$$H^2 = \frac{8\pi G}{3} \rho - \frac{f}{6} + \frac{T f_T}{3}, \quad (7)$$

$$\dot{H} = - \left[ \frac{4\pi G(\rho + p)}{1 + f_T + 2T f_{TT}} \right], \quad (8)$$

where  $H \equiv \dot{a}/a$  denote the Hubble parameter and dots represent the derivative with respect to time and  $\rho$  and  $p$  be the energy density and pressure of the matter content and  $T = -6H^2$ . From equations (7) and (8), we obtain the expressions of density  $\rho$ , pressure  $p$  and EoS parameter  $\omega$  respectively as

$$\rho = 3H^2 + \frac{f}{2} + 6H^2 f_T \quad (9)$$

$$p = -2\dot{H}(1 + f_T - 12H^2 f_{TT}) - (3H^2 + \frac{f}{2} + 6H^2 f_T) \quad (10)$$

$$\omega = \frac{p}{\rho} = -1 - \frac{2\dot{H}(1 + f_T - 12H^2 f_{TT})}{(3H^2 + \frac{f}{2} + 6H^2 f_T)} \quad (11)$$

where we set  $8\pi G = 1$ . Furthermore, the continuity equation reads

$$\dot{\rho} + 3H(1 + \omega)\rho = 0, \quad (12)$$

### III. KINEMATIC VARIABLES

The system of field equations described above has only two independent equations with four unknowns. To solve the system completely and in order to study the temporal evolution of energy density, pressure and EoS parameter, we need two more constraint equations (extra conditions). In literature, there are several arguments to choose these equations (see [18] for details). The method is well known as the model independent way approach to study cosmological models that generally considers a parametrizations of any kinematic variables such as Hubble parameter, deceleration parameter, jerk parameter and EoS parameter and provide the necessary supplementary equation [19]. Bearing that in mind, we shall work with a parametrization of deceleration parameter proposed in [20] as

$$q = -1 + \alpha \left[ -1 + \frac{1}{1 + \left(\frac{1}{1+z}\right)^\alpha} \right] \quad (13)$$

where  $\alpha$  shall be constrained from a chi-square test using any observational datasets (ref. section VII). The motivation use this parametrization is driven by the fact that equation (13) allows a signature flipping for  $-1 > \alpha > -2$ . Additionally note that

- $\alpha = -2$  corresponds to a decelerated universe at  $z = 0$ .
- $\alpha < -2$  corresponds to an accelerated universe in the future (i.e.,  $z < 0$ ).
- $\alpha \geq -1$  corresponds to an externally accelerating universe.

The expression of Hubble parameter for the parametrization (13) reads

$$H = \beta \left[ 1 + \left( \frac{1}{1+z} \right)^\alpha \right] \quad (14)$$

where  $\beta$  is the integration constant. To obtain (14), we used the relation

$$\frac{H(z)}{H_0} = \exp \left[ \int_0^z \frac{1 + q(z')}{1 + z'} dz' \right] \quad (15)$$

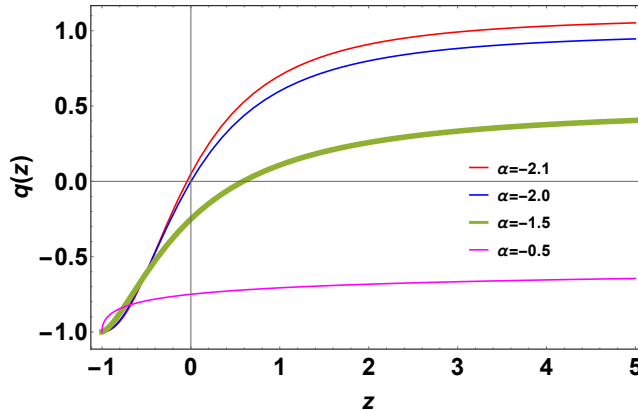


FIG. 1: Plot of deceleration parameter ( $q$ ) as a function of redshift ( $z$ ) for different values of model parameter  $\alpha$  showing diverge evolutionary dynamics.

Higher order derivatives of deceleration parameter such as jerk ( $j$ ), snap ( $s$ ) and lerk ( $l$ ) parameters provide important information about the evolution of the universe. They are represented as [21]

$$j(z) = (1+z) \frac{dq}{dz} + q(1+2q),$$

$$s(z) = -(1+z) \frac{dj}{dz} - j(2+3q),$$

$$l(z) = -(1+z) \frac{ds}{dz} - s(3+4q)$$

The jerk parameter represents the evolution of deceleration parameter. Since  $q$  can be constrained from observations, jerk parameter is used to predict the future. Additionally, the jerk parameter along with higher derivatives such as snap and lerk parameters provide useful insights into the emergence of sudden future singularities [21]. From Fig. 2 and Fig. 4, the jerk and lerk parameters are observed to have decreasing behaviors. Also, as the value of  $\alpha$  decreases, the parameters assumes higher values at redshift  $z = 0$ . Both of these parameters are positive which represents an accelerated expansion. The snap parameter is negative for all  $\alpha$  which also denote an accelerated expansion. Interestingly, the jerk parameter does not attain unity at  $z = 0$  which clearly does not coincide with  $\Lambda$ CDM model. Interestingly, this implies that the late time acceleration can be caused due to modifications of gravity. It is therefore encouraging to study the dynamics of EoS parameter which may arise purely due to geometric effects in the framework of modified gravity theories such as teleparallel gravity.

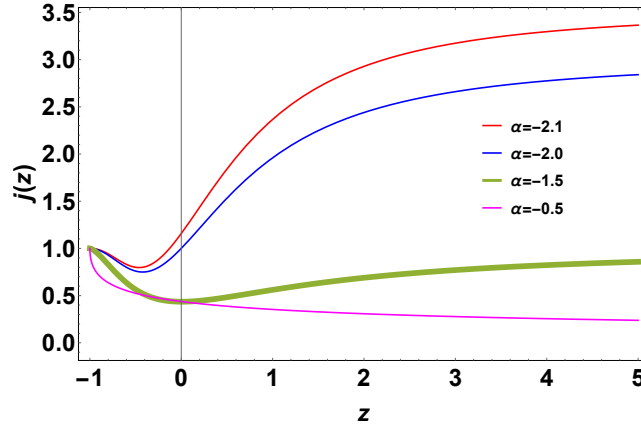


FIG. 2: Jerk parameter as a function of redshift.

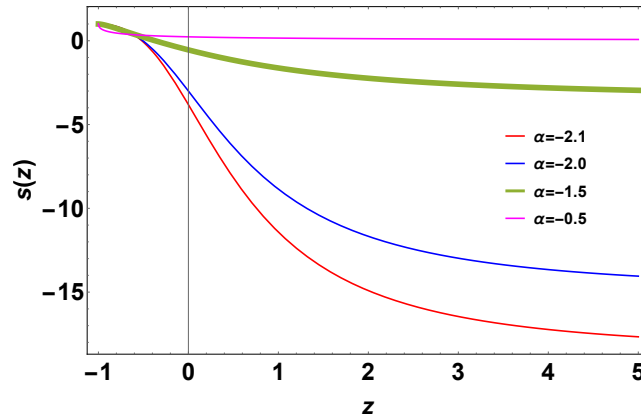


FIG. 3: Snap parameter as a function of redshift.

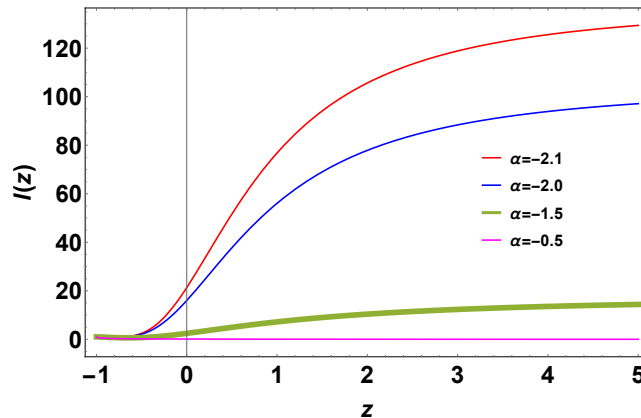


FIG. 4: Lerk parameter as a function of redshift.

## IV. COSMOLOGY WITH TELEPARALLEL GRAVITY

### A. Hybrid Teleparallel Gravity

For the first case, we presume the functional form of teleparallel gravity to be

$$f(T) = e^{mT}T^n, \quad (16)$$

where  $m \geq 0$  and  $n$  constants. Interestingly, this model takes power-law and exponential forms depending on the values of  $n$  and  $m$ . Particularly:

- For  $m = 0$  Eq. (16) reduces to  $f(T) = T^n$  (power law).
- For and  $n = 0$ , Eq. (16) reduces to  $f(T) = e^{mT}$  (exponential).

Using Eq. (16) in Eq. (7) and Eq. (8), the expressions of energy density  $\rho$ , pressure  $p$  and EoS parameter  $\omega$  reads respectively as

$$\rho = 3K + 6^n(-K)^n e^{-6mK} \left( \frac{1}{2} - n + 6nK \right), \quad (17)$$

$$p = -2 \left( \alpha K - \frac{e^{-t\alpha\beta} \alpha \beta^2}{-1 + e^{-t\alpha\beta}} \right) \times \left\{ -1 + (-6K)^n e^{-6mK} \left[ m + 4mn - 12Km^2 - \frac{n}{6K} - \frac{n(n-1)}{3K} \right] \right\} \\ - 3K - 6^n(-K)^n e^{-6mK} \left( \frac{1}{2} - n + 6nK \right) \quad (18)$$

$$\omega = -1 - 2 \left( \alpha K - \frac{e^{-t\alpha\beta} \alpha \beta^2}{-1 + e^{-t\alpha\beta}} \right) \times \left\{ -1 + (-6K)^n e^{-6mK} \left[ m + 4mn - 12Km^2 - \frac{n}{6K} - \frac{n(n-1)}{3K} \right] \right\} \\ \times \left\{ 3K + 6^n(-K)^n e^{-6mK} \left( \frac{1}{2} - n + 6nK \right) \right\}^{-1} \quad (19)$$

where  $K = \frac{e^{-2t\alpha\beta} \beta^2}{(-1 + e^{-t\alpha\beta})^2}$ .

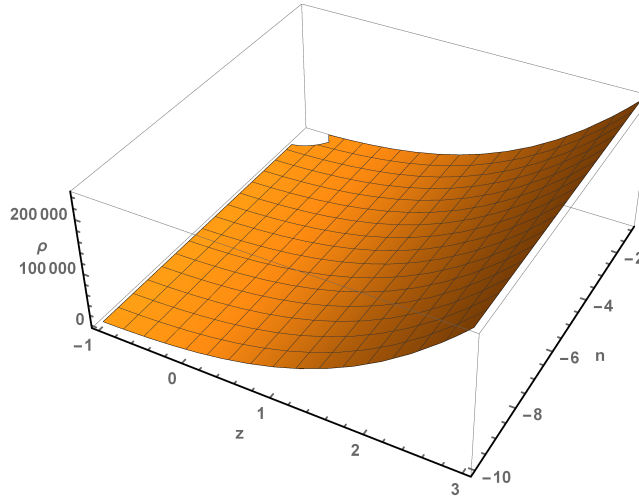


FIG. 5: Energy density as a function of redshift for  $\alpha = -1.5, \beta = 31.7455$  &  $m = 0.00155$ .

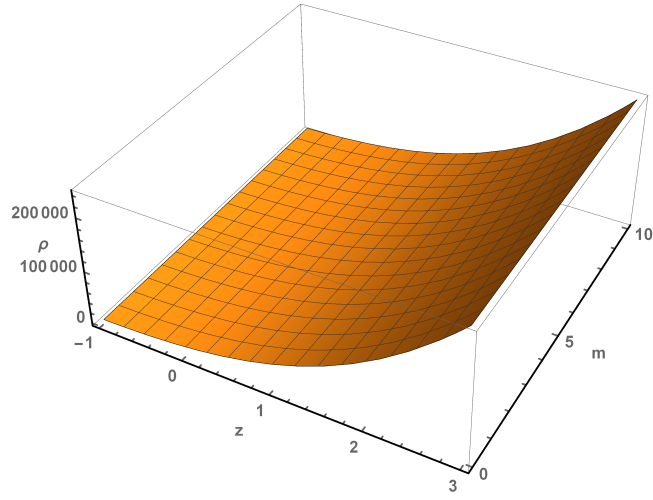


FIG. 6: Energy density as a function of redshift for  $\alpha = -1.5, \beta = 31.7455$  &  $n = 5$ .

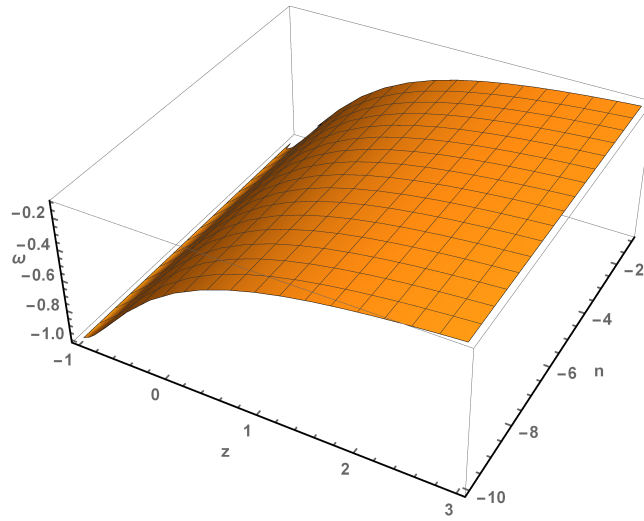


FIG. 7: EoS parameter as a function of redshift for  $\alpha = -1.5, \beta = 31.7455$  &  $m = 0.00155$ .

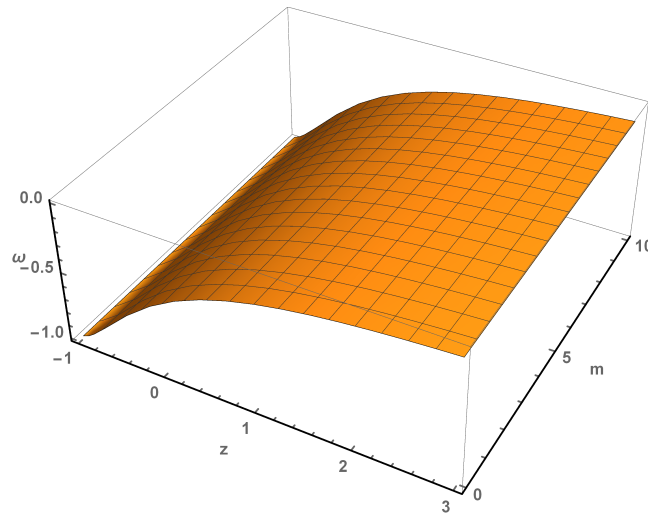


FIG. 8: EoS parameter as a function of redshift for  $\alpha = -1.5, \beta = 31.7455$  &  $n = 5$ .

### B. Logarithmic Teleparallel Gravity

For the second case, we presume the functional form of teleparallel gravity to be

$$f(T) = D \log(bT), \quad (20)$$

where  $D$  and  $b < 0$  are constants.

Using Eq. (20) in Eq. (7) and Eq. (8), the expressions of energy density  $\rho$ , pressure  $p$  and EoS parameter  $\omega$  reads respectively as

$$\rho = -D + 3K + \frac{D}{2} \log(6bK), \quad (21)$$

$$p = D - 3K - 2 \left(1 + \frac{D}{6K}\right) \left(\alpha K - \frac{e^{-t\alpha\beta} \alpha \beta^2}{-1 + e^{-t\alpha\beta}}\right) - \frac{D}{2} \log(6bK), \quad (22)$$

$$\omega = -1 - 2 \left(1 + \frac{D}{6K}\right) \left(\alpha K - \frac{e^{-t\alpha\beta} \alpha \beta^2}{-1 + e^{-t\alpha\beta}}\right) \times \left\{-D + 3K + \frac{D}{2} \log(6bK)\right\}^{-1} \quad (23)$$

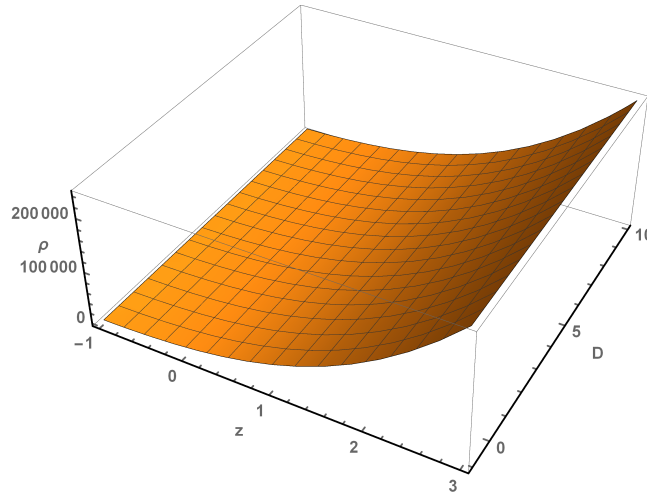


FIG. 9: Energy density as a function of redshift for  $\alpha = -1.5, \beta = 31.7455$  &  $b = -2$ .

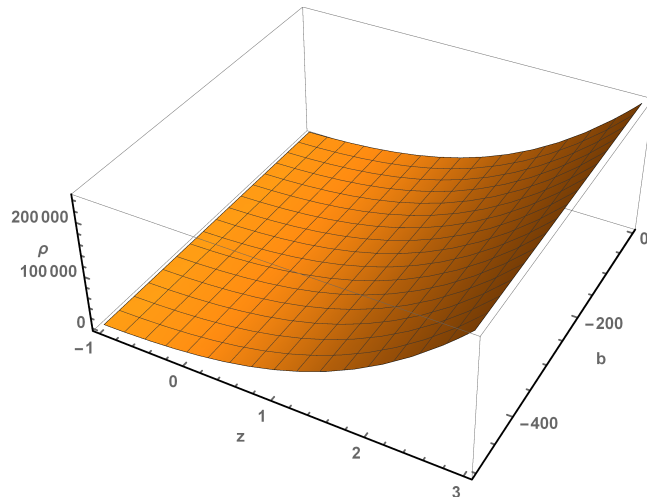


FIG. 10: Energy density as a function of redshift for  $\alpha = -1.5, \beta = 31.7455$  &  $D = 0.2$ .

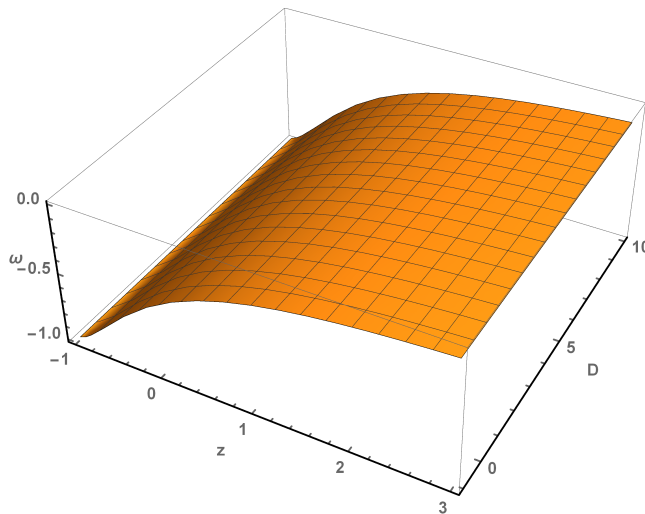


FIG. 11: EoS parameter as a function of redshift for  $\alpha = -1.5, \beta = 31.7455$  &  $b = -2$ .

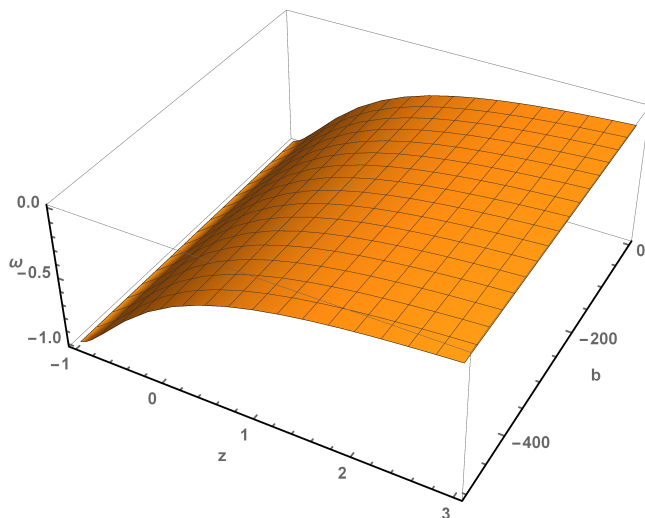


FIG. 12: EoS parameter as a function of redshift for  $\alpha = -1.5, \beta = 31.7455$  &  $D = 0.2$ .

## V. GEOMETRICAL DIAGNOSTICS

### A. Statefinder Diagnostics

Due to the fact that the number of dark energy models are quite large and increasing on a daily basis, it becomes absolutely necessary to find a method to distinguish a particular model from the well established DE models like the  $\Lambda$ CDM, SCDM, HDE, CG and Quintessence. With that reasoning, [22] proposed the  $\{r, s\}$  diagnostics where  $r$  and  $s$  are defined as

$$r = \frac{\ddot{a}}{aH^3},$$

$$s = \frac{r-1}{3\left(q-\frac{1}{2}\right)}, \left(q \neq \frac{1}{2}\right).$$

Different combinations of  $r$  and  $s$  represent different dark energy models. Particularly:

- For  $\Lambda$ CDM  $\rightarrow (r = 1, s = 0)$ .
- For SCDM  $\rightarrow (r = 1, s = 1)$ .



- For HDE  $\rightarrow (r = 1, s = \frac{2}{3})$ .
- For CG  $\rightarrow (r > 1, s < 0)$ .
- For Quintessence  $\rightarrow (r < 1, s > 0)$ .

The idea behind  $\{r, s\}$  diagnostics tool is that different dark energy models exhibit different trajectories in the  $\{r, s\}$  plane. The deviation from the point  $\{r, s\} = \{0, 1\}$  represent deviation from the well agreed  $\Lambda$ CDM model. Furthermore, the values of  $r$  and  $s$  could in principle be inferred from observations [23] and therefore could be very useful in discriminating dark energy models in the near future.

The expression of  $r$  and  $s$  parameters for our model reads

$$r = 1 + \frac{\alpha \left(\frac{1}{1+z}\right)^\alpha \left\{3 + \alpha + \left(\frac{1}{1+z}\right)^\alpha (3 + 2\alpha)\right\}}{\left\{1 + \left(\frac{1}{1+z}\right)^\alpha\right\}^2} \quad (24)$$

$$s = \frac{\alpha}{3} \left\{ -2 + \frac{1}{1 + \left(\frac{1}{1+z}\right)^\alpha} + \frac{3}{3 + \left(\frac{1}{1+z}\right)^\alpha (3 + 2\alpha)} \right\} \quad (25)$$

In Fig. 13, the  $\{r, s\}$  plane is shown for the parametrization (13) where the arrows indicate the direction of temporal evolution. The model is observed to deviate significantly from the point  $(0, 1)$  initially and is extremely sensitive to the value of  $\alpha$ . For  $\alpha \leq -2$ , the model initially starts its journey from the territory of Chaplygin gas ( $r > 1, s < 0$ ) and approaches towards  $\Lambda$ CDM at late times. For  $\alpha > -1$ , the model at high redshifts stays in the Quintessence region but again approaches towards  $\Lambda$ CDM. Interestingly, for  $\alpha = -1.5 \sim -1.5$  which is the chi-square value, we observed at high redshifts, the model to be very close to the point  $(r = 1, s = \frac{2}{3})$  which is the region of HDE. However, at late times the model is observed to coincide with  $(r = 1, s = 0)$ . Therefore, the parametrization used in this work is interesting and warrants further attention.

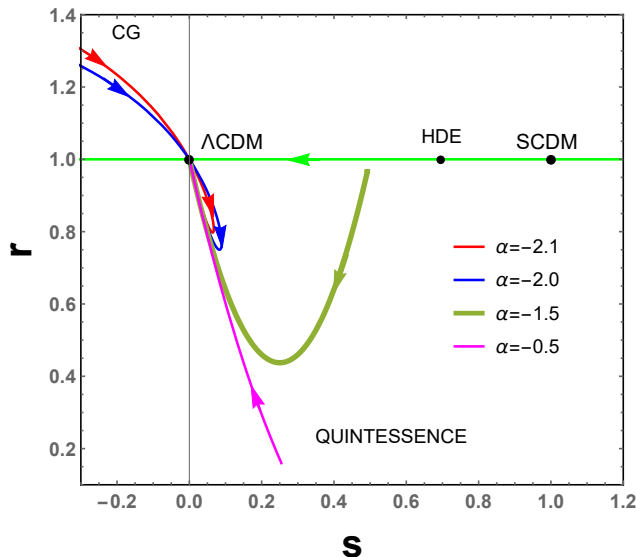


FIG. 13:  $\{r, s\}$  plane for the redshift range  $z[-1, 5]$  for different values of  $\alpha$ .

In addition to the  $\{r, s\}$  plane, we construct the  $\{r, q\}$  plane to get additional understanding of the parametrization (13). In  $\{r, q\}$  plane, the solid line in the middle represents the evolution of the  $\Lambda$ CDM universe and also divide the plane into two sections. The upper section belong to Chaplygin gas models and the lower section to Quintessence models.

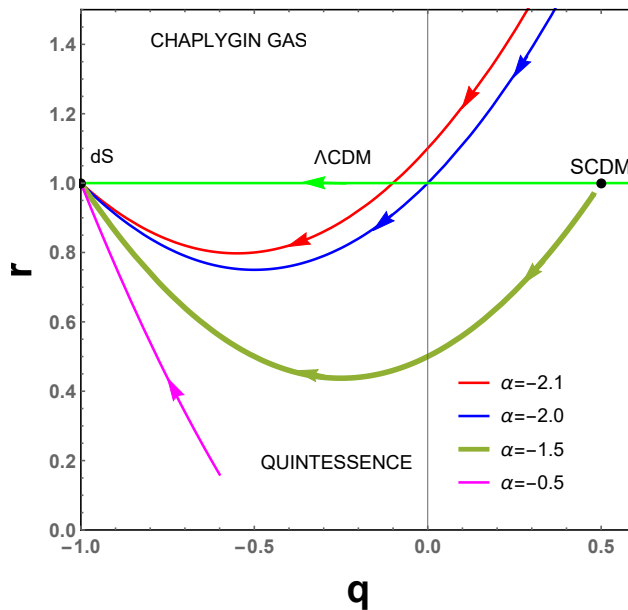


FIG. 14:  $\{r, q\}$  plane for the redshift range  $z[-1, 5]$  for different values of  $\alpha$ .

We observe from Fig. 14, that except for  $\alpha = -0.5$ , all the profiles starts from  $r > 1, q > 0$  which is very close to SCDM universe, followed by the region  $r < 1, -1 < q < 0$  and finally approaches the de-Sitter expansion with  $r = 1, q = -1$ . However, for  $\alpha < -1$ ,  $q$  is always negative and therefore the profile does not start from the SCDM universe.

### B. $Om$ Diagnostic

Another very useful diagnostic tool constructed from the Hubble parameter is the  $Om$  diagnostic which essentially provide a null test of the  $\Lambda$ CDM model [24]. This tool easily captures the dynamical nature of dark energy models from the slope of  $Om(z)$ . If the slope of this diagnostic tool were to be positive, it would imply a Quintessence nature ( $\omega > -1$ ) whereas the opposite would prefer a Phantom nature ( $\omega < -1$ ). Interestingly, only when the nature of the dark energy model coincide with that of the cosmological constant ( $\omega = -1$ ), the slope is constant with respect to redshift. It is defined as

$$Om(z) = \frac{\left(\frac{H(z)}{H_0}\right)^2 - 1}{z^3 + 3z^2 + 3z} \quad (26)$$

From Fig. 15, we observe a negative slope for  $\alpha > -2$  and therefore represents a dark energy model which is Phantom in nature. Nonetheless, for  $\alpha \leq -2$ ,  $Om(z)$  increases with redshift and therefore represents an Quintessence dark energy model. Hence, the value of  $\alpha$  dictates the nature of the underlying dark energy model represented by the parametrization (13).

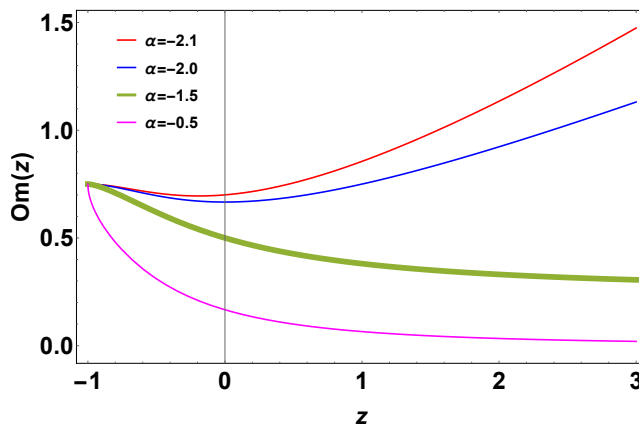


FIG. 15:  $Om(z)$  for different values of  $\alpha$ .

## VI. ENERGY CONDITIONS

Based upon the Raychaudhuri equation, the energy conditions are essential to describe the behavior of the compatibility of timelike, lightlike or spacelike curves [25] and often used to understand the dreadful singularities [26]. Energy conditions in teleparallel gravity have been studied in [27]. Energy conditions also provide the corners in parameter spaces since they violate, for instance, in presence of singularities. They are defined as:

- Strong energy conditions (SEC): Gravity is always attractive and therefore  $\rho + 3p \geq 0$ ;
- Weak energy conditions (WEC): Energy density should always be positive, i.e.,  $\rho \geq 0, \rho + p \geq 0$ ;
- Null energy condition (NEC): Minimum requirement for the fulfilment of SEC and WEC, i.e.,  $\rho + p \geq 0$ ;
- Dominant energy conditions (DEC): Energy density is always positive and independent of the observer's reference frame, i.e.,  $\rho \geq 0, |p| \leq \rho$ .

Energy conditions for both the teleparallel gravity models are presented in Fig. 16-17.

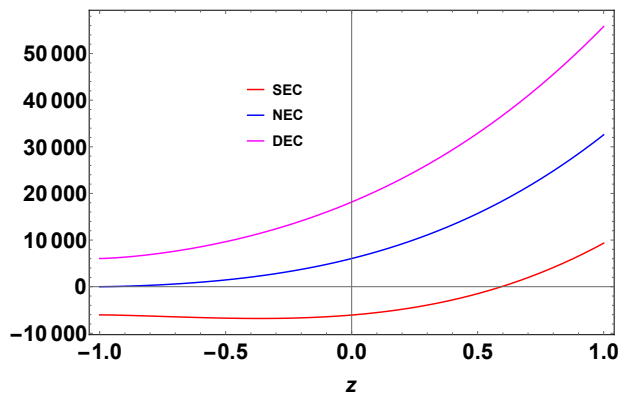


FIG. 16: ECs as a function redshift  $z$  for  $\beta = 31.7455, \alpha = -1.5, m = 0.00155$  &  $n = -5$  for hybrid teleparallel gravity.

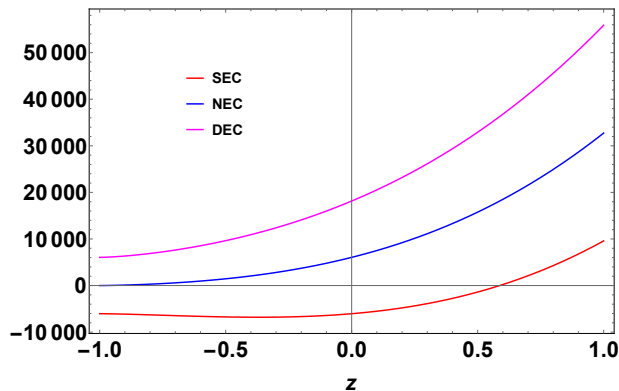


FIG. 17: ECs as a function redshift  $z$  for  $\beta = 31.7455, \alpha = -1.5, b = -2$  &  $d = 0.2$  for logarithmic teleparallel gravity.

## VII. OBSERVATIONAL CONSTRAINTS

In order to find the best fit value of the model parameters of our obtained models, we need to constrain the parameters with some available datasets. Here, we use three datasets, namely, Hubble datasets with 57 datapoints, Supernovae datasets consisting of 580 data points from Union2.1 compilation datasets and Baryonic Acoustic Oscillation (BAO) datasets. We use the Bayesian statistics for our analysis.

### A. Hubble parameter $H(z)$

Recently, Sharov and Vasiliev [28] compiled a list of 57 points of measurements of the Hubble parameter at in the redshift range  $0.07 \leq z \leq 2.42$ , measured by extraction of  $H(z)$  from line-of-sight BAO data including the analysis

of correlation functions of luminous red galaxies [29] and  $H(z)$  estimations from differential ages  $\Delta t$  of galaxies (DA method) [30]. (See the Appendix in [28] for full list of tabulated datasets). Chi square test is used to constrain the model parameters parameters given by

$$\chi_{OHD}^2(p_s) = \sum_{i=1}^{57} \frac{[H_{th}(p_s, z_i) - H_{obs}(z_i)]^2}{\sigma_{H(z_i)}^2} \quad (27)$$

where  $H_{th}(p_s, z_i)$  denotes the Hubble parameter at redshift  $z_i$  predicted by the models with  $p_s$  denoting the parameter space ( $\alpha$  here in our model),  $H_{obs}(z_i)$  is the  $i$ -th measured one and  $\sigma_{H(z_i)}$  is its uncertainty. We also take a prior as  $H_0 = 67.8$  (Planck result predicted value) for our analysis.

## B. Type Ia Supernova

Further we consider, the 580 points of Union2.1 compilation supernovae datasets [31] for our analysis for which the chi square formula is given as,

$$\chi_{SN}^2(\mu_0, p_s) = \sum_{i=1}^{580} \frac{[\mu_{th}(\mu_0, p_s, z_i) - \mu_{obs}(z_i)]^2}{\sigma_{\mu(z_i)}^2}, \quad (28)$$

where  $\mu_{th}$  and  $\mu_{obs}$  are correspondingly the theoretical and observed distance modulus for the model and the standard error is  $\sigma_{\mu(z_i)}$ . The distance modulus  $\mu(z)$  is defined to be  $\mu(z) = m - M = 5 \text{Log} D_l(z) + \mu_0$ , where  $m$  and  $M$  are the apparent and absolute magnitudes of any standard candle (supernovae of type *Ia* here) respectively. Luminosity distance  $D_l(z)$  and the nuisance parameter  $\mu_0$  are given by  $D_l(z) = (1+z)H_0 \int_0^z \frac{1}{H(z^*)} dz^*$  and  $\mu_0 = 5 \text{Log} \left( \frac{H_0^{-1}}{Mpc} \right) + 25$  respectively. In order to calculate luminosity distance, we have restricted the series of  $H(z)$  up to tenth term only and then integrated the approximate series to obtain the luminosity distance.

## C. Baryon Acoustic Oscillations

Finally, we consider a sample of BAO distances measurements from surveys of SDSS(R) [32], 6dF Galaxy survey [33], BOSS CMASS [34] and three parallel measurements from WiggleZ [35]. In the context of BAO measurements, the distance redshift ratio  $d_z$  is given as,

$$d_z = \frac{r_s(z_*)}{D_v(z)}, \quad (29)$$

where  $r_s(z_*)$  is the co-moving sound horizon at the time photons decouple and  $z_*$  indicates the photons decoupling redshift i.e.  $z_* = 1090$  [36]. Moreover,  $r_s(z_*)$  is assumed same as considered in the reference [37] together with the dilation scale is given by  $D_v(z) = \left( \frac{d_A^2(z) z}{H(z)} \right)^{\frac{1}{3}}$ , where  $d_A(z)$  is the angular diameter distance. The  $\chi_{BAO}^2$  values corresponding to BAO measurements are discussed in details in [38] and the chi square formula is given by,

$$\chi_{BAO}^2 = A^T C^{-1} A, \quad (30)$$

where the matrix  $A$  is given by

$$A = \begin{bmatrix} \frac{d_A(z_*)}{D_v(0.106)} - 30.84 \\ \frac{d_A(z_*)}{D_v(0.35)} - 10.33 \\ \frac{d_A(z_*)}{D_v(0.57)} - 6.72 \\ \frac{d_A(z_*)}{D_v(0.44)} - 8.41 \\ \frac{d_A(z_*)}{D_v(0.6)} - 6.66 \\ \frac{d_A(z_*)}{D_v(0.73)} - 5.43 \end{bmatrix},$$

and  $C^{-1}$  representing the inverse of covariance matrix  $C$  given as in the reference [38] adopting the correlation coefficients presented in [39] as

$$C^{-1} = \begin{bmatrix} 0.52552 & -0.03548 & -0.07733 & -0.00167 & -0.00532 & -0.00590 \\ -0.03548 & 24.97066 & -1.25461 & -0.02704 & -0.08633 & -0.09579 \\ -0.07733 & -1.25461 & 82.92948 & -0.05895 & -0.18819 & -0.20881 \\ -0.00167 & -0.02704 & -0.05895 & 2.91150 & -2.98873 & 1.43206 \\ -0.00532 & -0.08633 & -0.18819 & -2.98873 & 15.96834 & -7.70636 \\ -0.00590 & -0.09579 & -0.20881 & 1.43206 & -7.70636 & 15.28135 \end{bmatrix}.$$

Below, we have shown a comparison of our obtained model with the  $\Lambda$ CDM model together with error bars due to the 57 points of  $H(z)$  datasets and the 580 points of Union2.1 compilation datasets.

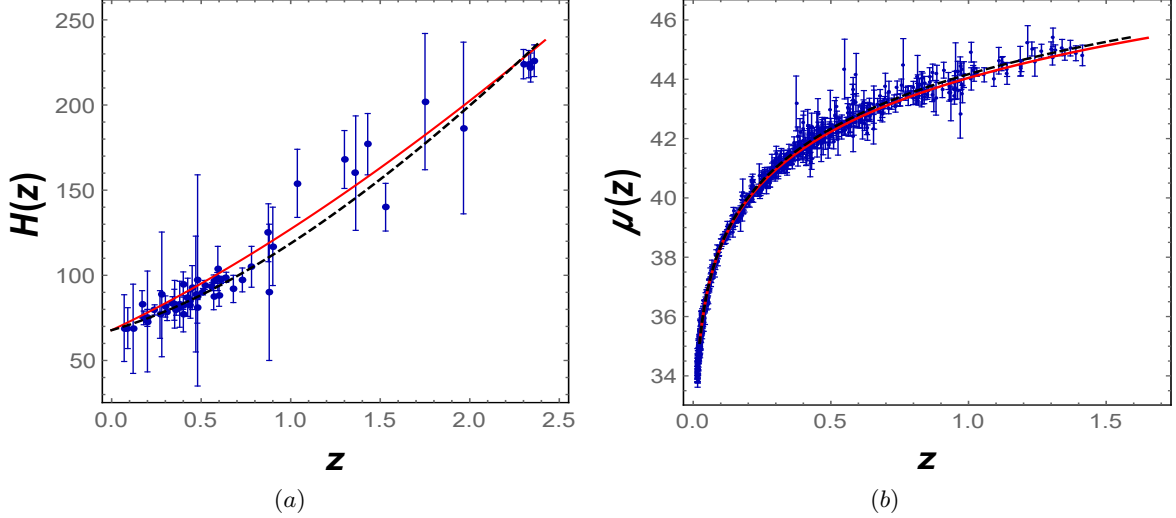


FIG. 18: Figures (a) and (b) are respectively the error bar plots of 57 points of  $H(z)$  datasets and 580 points of Union2.1 compilation supernovae datasets together with our obtained model (solid red lines) and  $\Lambda$ CDM model (black dashed lines).

Next, we have shown the likelihood contours for the model parameter  $\alpha$  and Hubble constant  $H_0$  with errors at  $1-\sigma$ ,  $2-\sigma$  and  $3-\sigma$  levels in the  $\alpha$ - $H_0$  plane. The best fit constrained values of  $\alpha$  and  $H_0$  are found to be  $\alpha = -1.497294$  &  $H_0 = 63.490604$  due to  $H(z)$  datasets only with  $\chi^2_{\min} = 31.333785$  and  $\alpha = -1.503260$  &  $H_0 = 63.361612$  due to joint datasets  $H(z) + SNeIa + BAO$  with  $\chi^2_{\min} = 650.312968$  respectively.

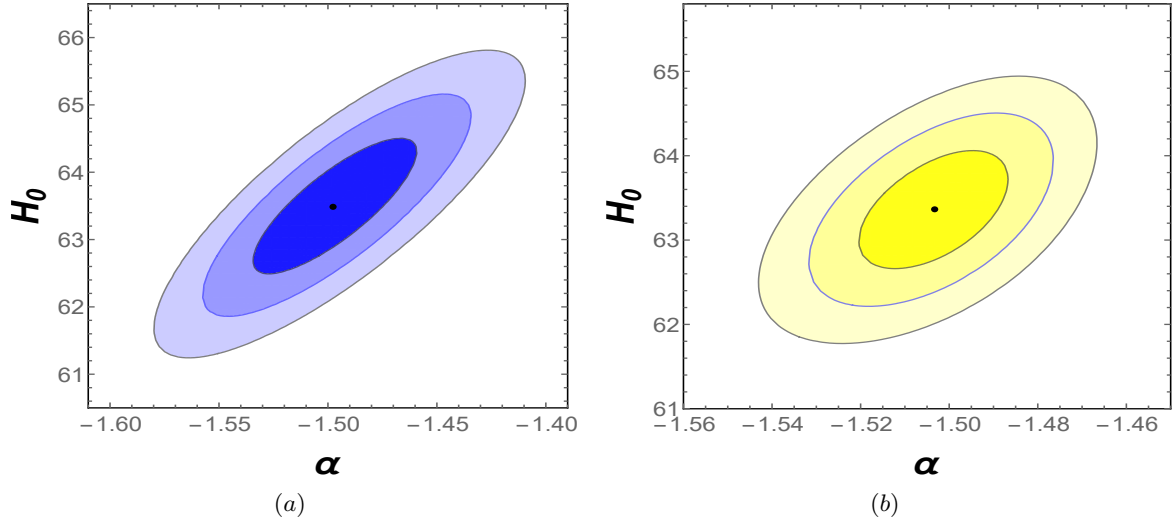


FIG. 19: Figures (a) shows the maximum likelihood contours in the  $\alpha$ - $H_0$  plane for  $H(z)$  datasets only while figure (b) shows the maximum likelihood for  $H(z) + SNeIa + BAO$  datasets jointly. The three contour regions shaded with dark, light shaded and ultra lightshaded in both the plots are with errors at  $1-\sigma$ ,  $2-\sigma$  and  $3-\sigma$  levels. The black dots represent the best fit values of model parameter  $\alpha$  and  $H_0$  in both the plots.

## VIII. RESULTS AND DISCUSSIONS

The manuscript communicates the phenomena of late time acceleration in the framework of hybrid and logarithmic teleparallel gravity. To obtain the exact solutions of the field equations, we employ a parametrization of deceleration parameter first proposed in [20]. In this section, we shall discuss the energy conditions and the cosmological viability of the underlying teleparallel gravity models.

In Section VI, we show the temporal evolution of SEC, NEC and WEC for both the teleparallel gravity models. Note that in order to suffice the late time acceleration, the SEC has to violate [40]. This is due to the fact that for an accelerating universe compatible with observations [1], the EoS parameter  $\omega \simeq -1$  [41], and therefore  $\rho(1 + 3\omega) < 0$  always. From Fig.16-17, one can clearly observe that SEC violate for both the models whereas NEC and WEC do not violate. Interestingly, SEC is also violated for curvature coupled and minimally coupled scalar field theories [40]. To understand the cosmological viability of both the teleparallel gravity models, we show in Fig. 1, the deceleration parameter ( $q$ ) as a function of redshift. The plot of the deceleration parameter  $q(z)$  clearly shows that our model successfully generates late time cosmic acceleration along with a decelerated expansion in the past for  $-1 > \alpha > -2$ . The deceleration parameter undergoes a signature flipping at the redshift  $z_{tr} \simeq 0.6$  for the chi-square value of  $\alpha = -1.5$  which is compatible with latest Planck measurements [41]. Our values of  $q_0 = -0.251355$  and  $z_{tr}$  are consistent with values reported by other authors [42]. From Figs. 8 & 12 the values of EoS  $\omega$  at  $z = 0$  for both our models are obtained as  $-0.500903$  and  $-0.500935$  respectively. These values of  $\omega$  behave in concordance with standard cosmological model predictions (with Planck data,  $\omega_{eff}^{LCDM} \sim -0.68$  at  $z = 0$  as in Ref. [41]).

In Fig. 5,6,9 and 10, we plot the energy density for both the models as a function of redshift. We chose the model parameters so as to satisfy the WEC. Fulfillment of WEC ensures the cosmological pressure has to be negative to account for negative EoS parameter and therefore the cosmic acceleration. It is interesting to note that no known entity has the remarkable property of negative pressure and can only be achieved by exotic matter or by modifications to general relativity.

The EoS parameter is an important cosmological parameter which has sparked great deal of interest among cosmologists. Owing to the mysterious nature of the cosmological entity responsible for this acceleration, various dark energy models have been devised to suffice the observations. To investigate the nature of the dark energy model represented by the equation (13), we study in Section VI, the  $\{r, s\}$  and  $\{r, q\}$  plane and  $Om(z)$ . We observe that the value of  $\alpha$  dictates the evolution of the  $r$ - $s$  and  $r$ - $q$  trajectories. We find the model to deviate significantly from the  $\Lambda$ CDM at early times. However, at late times the model is observed to coincide with ( $r = 1, s = 0$ ) and therefore consistent with  $\Lambda$ CDM cosmology. This result is further re-assured from the  $r$ - $q$  plane in Fig. 14. However, discrepancy arises from Fig. 15, where for none of the values of  $\alpha$  we obtain a constant  $Om$  which clearly does not reflect a dark energy which is time independent. Furthermore, the nature of dark energy represented by the equation (13) changes from being an Quintessence to Phantom as  $\alpha$  changes from  $\alpha \leq -2$  to  $\alpha > -2$  respectively. Finally, we have discussed our obtained models in the light of some observational datasets. The obtained model has a nice fit to the 57 points of Hubble datasets and the 580 points of Union2.1 compilation supernovae datasets. We have used the Bayesian statistics to find the constraints on the model parameters. The maximum likelihood contours for the model parameter  $\alpha$  and Hubble constant  $H_0$  with errors at  $1\text{-}\sigma$ ,  $2\text{-}\sigma$  and  $3\text{-}\sigma$  levels in the  $\alpha$ - $H_0$  plane is shown separately for  $H(z)$  datasets only and joint datasets  $H(z) + SNeIa + BAO$ . The best fit constrained values of  $\alpha$  and  $H_0$  are found to be  $\alpha = -1.497294$  &  $H_0 = 63.490604$  due for  $H(z)$  datasets with  $\chi_{\min}^2 = 31.333785$  and  $\alpha = -1.503260$  &  $H_0 = 63.361612$  due to  $H(z) + SNeIa + BAO$  datasets with  $\chi_{\min}^2 = 650.312968$  respectively.

### Acknowledgments

S.M. acknowledges Department of Science & Technology (DST), Govt. of India, New Delhi, for awarding Junior Research Fellowship (File No. DST/INSPIRE Fellowship/2018/IF180676). SB thanks Biswajit Pandey for helpful discussions. PKS acknowledges CSIR, New Delhi, India for financial support to carry out the Research project [No.03(1454)/19/EMR-II Dt.02/08/2019]. We are very much grateful to the honorable referee and the editor for the illuminating suggestions that have significantly improved our work in terms of research quality and presentation.

- 
- [1] A. G. Riess et al., *Astron. J.* **116**, 1009 (1998); S. Perlmutter et al., *Astrophys. J.* **517**, 565 (1999); P. deBernardis et al., *Nature* **404**, 955 (2000); S. Perlmutter et al., *Astrophys. J.* **598**, 102 (2003); M. Colless et al., *Mon. Not. R. Astron. Soc.* **328**, 1039 (2001); M. Tegmark et al., *Phys. Rev. D* **69**, 103501 (2004); S. Cole et al., *Mon. Not. R. Astron. Soc.* **362**, 505 (2005); V. Springel et al., *Nature (London)* **440**, 1137 (2006); P. A. R. Ade et al., *Astron. Astrophys.* **571**, A16 (2014); P. Astier et al., *Astron. Astrophys.* **447**, 31 (2006); A. G. Riess et al., *Astrophys. J.* **659**, 98 (2007); D. N. Spergel et al., *Astrophys. J. Suppl. Ser.* **148**, 175 (2003); H. V. Peiris et al., *Astrophys. J. Suppl. Ser.* **148**, 213 (2003); D. N. Spergel et al., *Astrophys. J. Suppl. Ser.* **170**, 377 (2007); E. Komatsu et al., arXiv:0803.0547.
- [2] B. Ratra, P. J. E. Peebles, *Phys. Rev. D* **37**, 3406 (1988); R. R. Caldwell et al., *Phys. Rev. Lett.* **80**, 1582 (1988); C. Armendariz-Picon et al., *Phys. Rev. D* **63**, 103510 (2001); T. Buchert, *Gen. Relativ. Gravit.* **32**, 105 (2000); P. Hunt, S.

- Sarkar, Mon. Not. R. Astron. Soc. **401**, 547 (2010); K. Tomita, Mon. Not. R. Astron. Soc. **326**, 287 (2001); B. Pandey, Mon. Not. R. Astron. Soc. **485**, L73 (2019); B. Pandey, Mon. Not. R. Astron. Soc. **471**, L77 (2017); K. A. Milton, Gravit. Cosmol. **9**, 66 (2003); D. Easson et al., Phys. Lett. B **696**, 273 (2011); D. Pavón, N. Radicella, Gen. Relativ. Gravit. **45**, 63 (2013); N. Radicella, D. Pavón, Gen. Relativ. Gravit. **44**, 685 (2012).
- [3] A. Paliathanasis et al., Phys. Rev. D **94**, 023525 (2016).
- [4] S. Nojiri et al., Phys. Rept. **692**, 1 (2017).
- [5] P.K. Sahoo and S. Bhattacharjee, New Astronomy, **77**, 101351 (2020); R. Zaregonbadi, et al., Phys. Rev. D **94**, 084052 (2016); G. Sun and Y.-C. Huang, Int. J. Mod. Phys. D, **25**, 1650038 (2016); F. Rocha et al. arXiv:1911.08894 (2019); S.I. dos Santos, G.A. Carvalho, P.H.R.S. Moraes, C.H. Lenzi and M. Malheiro, Eur. Phys. J. Plus, **134**, 398 (2019); P.H.R.S. Moraes, J.D.V. Arbanil and M. Malheiro, J. Cosm. Astrop. Phys. **06**, 005 (2016); P.H.R.S. Moraes and P.K. Sahoo, Eur. Phys. J. C **79**, 677 (2019); E. Elizalde and M. Khurshudyan, Phys. Rev. D, **99**, 024051 (2019); P.H.R.S. Moraes, W. de Paula and R.A.C. Correa, Int. J. Mod. Phys. D, **28**, 1950098 (2019); E. Elizalde and M. Khurshudyan, Phys. Rev. D, **98**, 123525 (2018); P.H.R.S. Moraes and P.K. Sahoo, Phys. Rev. D, **97**, 024007 (2018); P.K. Sahoo, P.H.R.S. Moraes and P. Sahoo, Eur. Phys. J. C, **78**, 46 (2018); P.K. Sahoo, P.H.R.S. Moraes, P. Sahoo and G. Ribeiro, Int. J. Mod. Phys. D, **27**, 1950004 (2018); P.H.R.S. Moraes and P.K. Sahoo, Phys. Rev. D, **96**, 044038 (2017); P.H.R.S. Moraes, R.A.C. Correa and R.V. Lobato, J. Cosm. Astrop. Phys., **07**, 029 (2017); T. Azizi, Int. J. Theor. Phys. **52**, 3486 (2013); M. Sharif and A. Siddiq, Gen. Rel. Grav., **51**, 74 (2019); M.E.S. Alves, P.H.R.S. Moraes, J.C.N. de Araujo and M. Malheiro, Phys. Rev. D, **94**, 024032 (2016); P.K. Sahoo and S. Bhattacharjee, Int. J. Theor. Phys, DOI: 10.1007/s10773-020-04414-3 [arXiv: 1907.13460]; S. Bhattacharjee and P. K. Sahoo, Eur. Phys. J. C. **80**, 289 (2020) [arXiv: 2002.11483]; P. Sahoo et al, Mod. Phys. Lett. A, DOI: 10.1142/S0217732320500959 [arXiv: 1907.08682] ;S. Bhattacharjee and P. K. Sahoo, Phys. Dark universe. **28**, 100537 (2020) [arXiv: 2003.14211]; S. Bhattacharjee and P. K. Sahoo, Eur. Phys. J. Plus, **135**, 86 (2020) [arXiv:2001.06569]; S. Bhattacharjee and P. K. Sahoo, Eur. Phys. J. Plus, DOI: 10.1140/epjp/s13360-020-00361-4.
- [6] G. R. Bengochea, R. Ferraro, Phys. Rev. D **79**, 124019 (2009); R. Ferraro, F. Fiorini, Phys. Rev. D **75**, 084031 (2007); E. V. Linder, Phys. Rev. D **81**, 127301 (2010).
- [7] Y. F. Cai et al., Rept. Prog. Phys. **79**, no.4, 106901 (2016).
- [8] K. Hayashi, T. Shirafuji, Phys. Rev. D **19**, 3524 (1979); M. Tsampanlis, Phys. Lett. A **75**, 27 (1979); H. I. Arcos, J.G. Pereira, Int. J. Mod. Phys. D **13**, (2004) 2193
- [9] A. Einstein 1928, Sitz. Preuss. Akad. Wiss. p. 217; *ibid* p. 224 [Translated by A. Unzicker and T. Case, (preprint: arXiv: physics/0503046)]
- [10] M. E. Rodrigues et al., Astroph. Space Sci. **357**, 129 (2015)
- [11] A. Paliathanasis et al., Phys. Rev. D **89**, 104042 (2014); S. Capozziello et al., JHEP **89**, 02 039 (2013).
- [12] K. Atazadeh, F. Darabi, Eur. Phys. J. C **72**, 2016 (2012); S. Basilakos et al., Phys. Rev. D **88**, 103526 (2013).
- [13] K. Bamba et al., Phys. Rev. D **94**, 083513 (2016).
- [14] G. R. Bengochea, R. Ferraro, Phys. Rev. D **79**, 124019 (2009); K. Bamba et al., JCAP **01**, 021 (2011); R. Myrzakulov, Eur. Phys. J. C **71**, 1752 (2011).
- [15] Y.F. Cai et al., Class. Quant. Grav. **28**, 215011 (2011); J. de Haro, J. Amorós, J. Phys. Conf. Ser. **600**, 012024 (2015); J. de Haro, J. Amorós, PoS FFP14, 163 (2016); W. El Hanafy, G. G. L. Nashed, Int. J. Mod. Phys. D **26**, 1750154 (2017).
- [16] M. Zaeem-ul-HaqBhatti, Z.Yousaf, Sonia Hanif, Phys. Dark Univ.,**16**, 34 (2017).
- [17] M. Zaeem-ul-Haq Bhatti, Z.Yousaf, Sonia Hanif, Mod. Phys. Lett. A, **32**, 1750042 (2017).
- [18] S. K. J. Pacif et al., Int. J. Geom. Meth. Mod. Phys. **14**, 1750111 (2017).
- [19] M. Chevallier, D. Polarski, Int. J. Mod. Phys. D **10**, 213 (2001); Mod. Phys. Lett. A. **35**, 2050011 (2020); S. del Campo et al., Phys. Rev. D **86**, 083509 (2012); A. A. Mamon, K.Bamba, Eur. Phys. J. C **78**, 862 (2018).
- [20] N. Banerjee, S. Das, Gen. Relativ. Gravit. **37**, 1695 (2005).
- [21] S. Pan, A.Mukherjee, N.Banerjee, Mon. Not. R. Astron. Soc. **477**, 1, 1189 (2018).
- [22] V. Sahni, T. D. Saini, A. A. Starobinsky, U. Alam: JETP Lett. **77**, 201 (2003); U. Alam et al., Mon. Not. R. Astron. Soc. **344**, 1057 (2003).
- [23] J. Albert et al. [SNAP Collaboration]: arXiv:0507458; J. Albert et al. [SNAP Collaboration]: arXiv:0507459.
- [24] V. Sahni et al., Phys. Rev. D **78**, 103502 (2008); M. Shahalam1, Sasha Sami, Abhineet Agarwal, Mon. Not. Roy. Astron. Soc. **448** 2948 (2015); Abhineet Agarwal et al., Int. J. Mod. Phys. D**28** 1950083 (2019).
- [25] P. H. R. S. Moraes, P. K. Sahoo, Eur. Phys. J. C. **77**, 480 (2017).
- [26] R. M. Wald, General relativity (University of Chicago Press, Chicago, 1984)
- [27] D. Liu, M. J. Reboucas, Phys.Rev. D. **86**, 083515 (2012); T. Azizi, M. Gorjizadeh, EPL **117**, 6 (2017);M. Zubair, Saira Waheed, Astrophys Space Sci. **355**, 361 (2015).
- [28] G. S. Sharov, V. O. Vasiliev, Mathematical Modelling and Geometry, Vol. 6, No 1, 1 (2018).
- [29] C. H. Chuang, Y. Wang, Mon. Not. Roy. Astron. Soc. **435**, 255 (2013); C-H Chuang C-H. et al., Mon. Not. Roy. Astron. Soc. **433**, 3559 (2013); A. Font-Ribera et al., J. Cosmol. Astropart. Phys. **05**, 027 (2014); T. Delubac et al., Astron. Astrophys. **574**, id. A59, 17 (2015); L. Anderson et al., Mon. Not. Roy. Astron. Soc. **441**, 24 (2014); Y. Wang et al., Mon. Not. Roy. Astron. Soc. **469**, 3762 (2017); E. Gazta naga et al. Mon. Not. Roy. Astron. Soc. **399**, 1663 (2009); C. Blake et al., Mon. Not. Roy. Astron. Soc. **425**, 405 (2012); N. G. Busca et al., Astro. Astrophys. **552**, A96 (2013); A. Oka et al., Mon. Not. Roy. Astron. Soc. **439**, 2515 (2014); S. Alam et al., Mon. Not. Roy. Astron. Soc. **470**, 2617 (2017); J. E. Bautista et al., Astron. Astrophys. **603**, id. A12, 23 (2017).
- [30] J. Simon, L. Verde, R. Jimenez, Phys. Rev. D **71**, 123001 (2005); D. Stern et al., J. Cosmol. Astropart. Phys. **02**, 008 (2010); C. Zhang et al., Research in Astron. and Astrop. **14**, 1221 (2014); M. Moresco et al., J. Cosmol. Astropart. Phys. **8**, 006 (2012); M. Moresco, Mon. Not. Roy. Astron. Soc.: Letters., **450**, L16 (2015); M. Moresco M. et al., J. Cosmol. Astropart. Phys. **05**, 014 (2016); A. L. Ratsimbazafy et al., Mon. Not. Roy. Astron. Soc. **467**, 3239 (2017)
- [31] N. Suzuki *et al.*, Astrophys. J., **746** (2012) 85
- [32] N. Padmanabhan, X. Xu, D. J. Eisenstein, R. Scalzo, A. J. Cuesta, K. T. Mehta et al., Mon. Not. Roy. Astron. Soc. **427** (2012) 2132

- [33] F. Beutler, C. Blake, M. Colless, D. H. Jones, L. Staveley-Smith, L. Campbell et al., *Mon. Not. Roy. Astron. Soc.* **416** (2011) 3017
- [34] BOSS collaboration, L. Anderson et al., *Mon. Not. Roy. Astron. Soc.* **441** (2014) 24
- [35] C. Blake et al., *Mon. Not. Roy. Astron. Soc.* **425** (2012) 405
- [36] Ade P A R et al., Planck 2015 results. XIII. Cosmological parameters, Preprint arXiv:1502.01589 (2015)
- [37] M. Vargas dos Santos, Ribamar R. R. Reis, *J. Cosm. Astropart. Phys.*, **1602** (2016) 066
- [38] R. Giotri, M. V. d. Santos, I. Waga, R. R. R. Reis, M. O. Calvao and B. L. Lago, *JCAP* **1203** (2012) 027
- [39] G. Hinshaw et al., *Astrophys. J. Suppl.*, **208** (2013) 19
- [40] M. Visser, C. Barcelo. arXiv:gr-qc/0001099; C. Barcelo, M. Visser, *Int. J. Mod. Phys. D* **11**, 1553 (2002). arXiv:gr-qc/0205066
- [41] Planck Collaboration: arXiv:1807.06209.
- [42] B. S. Haridasu, V. V. Lukovic, M. Moresco, N. Vittorio, *J. Cosmol. Astropart. Phys.* **10**, 015 (2018); J. R. Garza et al., *Eur. Phys. J. C* **79**, 890 (2019); Hai-Nan Lin, Xin Li, Li Tang, *Chin. Phys. C* **43**, 075101 (2019); J. F. Jesus, R. Valentim, A. A. Escobal, S. H. Pereira, arXiv: 1909.00090.